Engineering

Electrical Engineering fields

Okayama University *Year* 1990

A single-phase PWM controlled AC to DC converter based on control of unity displacement power factor

Shigeyuki Funabiki
Okayama University

A Single-Phase PWM Controlled AC to DC Converter Based on Control of Unity Displacement Power Factor

Shigeyuki FUNABIKI
Dept. of Electrical and Electronic Engineering
Okayama University, Okayama 700, Japan

Abstract The new pulse width modulation (PWM) controlled AC to DC converter with a controllability of DC voltage and a high input power factor has been proposed. However, the displacement power factor and the input power factor become lower in the region of small current command. In this paper, the modified PWM control strategy in the single-phase AC to DC converter is proposed for the improvement of the displacement power factor and its characteristics are discussed analytically. The proposed PWM controlled AC to DC converter has an advantage of the high input power factor and the controllability of DC voltage from zero to more than the maximum value of the source voltage. The displacement power factor is unity in the whole range of current command. Then, the input power factor is almost unity in the wide range of current command.

INTRODUCTION

The PWM inverter is widely used as a variable voltage-variable frequency supply. The output voltage waveform of the inverter is desirable to be sinusoidal. However, it has a great deal of harmonics. Therefore, the methods of improving the output waveforms in the inverter have been proposed as follows;

1) a multiple inverter to superimpose the output voltage waveforms of some square-wave inverters
2) a PWM inverter with a modulation frequency of above 20 kHz [1]
3) a PWM inverter with the pulse pattern to optimize some specific performance criteria [2,3]
4) a PWM inverter with a fixed pulse pattern in combination with a pulse amplitude modulation (PAM) [4,5]

For the realization of the inverter in combination with PAM and PWM, it is necessary to develop a variable DC voltage supply. In general, the DC voltage is obtained by rectifying the AC voltage. Therefore, it is indispensable to develop the AC to DC converter with a controllability of DC voltage and an excellent input characteristics. Then, the authors have proposed a new AC to DC converter with a controllability of DC voltage from zero to more than the maximum value of the AC source voltage and an unity input power factor in the wide control range [6]. However, the filter current was not considered in the calculation of the current command. Then, the displacement power factor becomes lower under the current command 2.0 Amp. Further, the input power factor also becomes lower.

In this paper, a modified PWM control strategy in the single-phase AC to DC converter is proposed for the improvement of the displacement power factor and the input power factor and the input and output characteristics are discussed analytically. In this strategy, the pulse width is calculated taking account of the input filter current. Therefore, the displacement power factor is always unity in the whole range of current command. The input power factor is also improved by the proposed strategy. The proposed PWM controlled AC to DC converter has also an advantage of the high input power factor and the controllability of DC voltage from zero to more than the maximum value of the source voltage.

PWM CONTROLLED AC TO DC CONVERTER

Circuit Configuration

Fig. 1 shows a PWM controlled AC to DC converter

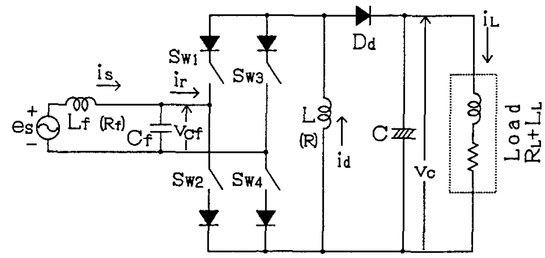

Fig. 1 PWM control AC to DC converter with input filter

with an input filter. The proposed converter is the application of the step-up and -down chopper to the AC to DC converter. The input filter absorbs the harmonics produced by the PWM performance of the converter in order to improve the waveform of the source current.

The performance of converter is same in the positive and the negative half cycle of the AC source voltage. Then, the performance of converter in the positive half cycle is described in the following. The switches S_{w2} and S_{w3} act in the period of the positive value of converter current command and the switches S_{w1} and S_{w4} act in the period of its negative value. The harmonics produced in the converter are filtered and the source current becomes a quasi-sinusoidal waveforms in phase with the AC source voltage.

Performance of Filter

The AC to DC converter observed from the AC stage can be considered to be a current source with a great deal of harmonics. Therefore, the equivalent circuit of the converter can be expressed as shown in Fig. 2. Neglecting the resistance of the filter reactor because of its little effect on its gain and phase characteristics, the transfer function of the filter is obtained by

$$G(j\omega) = \frac{1}{1 - (\omega/\omega_0)^2} \tag{1}$$

where
ω_0 $=1/\sqrt{L_f C_f}$
L_f an inductance of the input filter
C_f a capacitance of the input filter

In general, the angular resonant frequency of the input filter ω_0 is chosen a value of nine to ten times as many as the source angular frequency ω_s [7]. Thus, the most part of the fundamental component in the

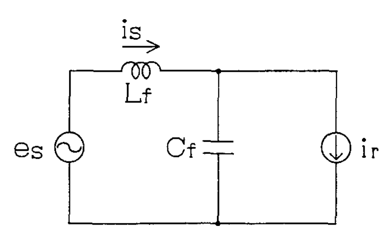

Fig. 2 Equivalent circuit of converter

90/CH 2935-5/90/0000-1012$01.00©1990 IEEE

current i_r is flowing into the source because the gain of the input filter $|G(j\omega_s)|$ is nearly 1.00. On the other hand, as the modulation angular frequency ($2n_p\omega_s$, n_p : the number of divisions in a half cycle of the AC source voltage) is selected to be sufficiently large compared with ω_0, the gain for the harmonics becomes less than several percent. Therefore, the harmonics hardly flows into the AC source.

Decision of Pulse Width

The source current i_s is the sum of the converter current i_r and the filter current i_f. The proposed control strategy is to make the fundamental component of source current in phase with the AC source voltage. The filter current is leading in 90 degrees to the AC source voltage. Therefore, in order to make the source current in phase with the AC source voltage, the source current I_{s1} should be derived as the vector sum of the converter current I_{r1} and the inverse filter current I_{f1} in regard to the fundamental component as shown in Fig. 3. Then, the converter current is the waveform with a lagging of θ degrees. In the proposed PWM strategy, the fundamental component of the source current is selected as the current command i_s^*. Then, the pulse width is calculated by using the converter current obtained from Fig. 3 as a converter current command i_r^*.

The on-time of the switches is decided as shown in Fig. 4. The half cycle of the source voltage is divided into n_p equal periods. One period Δt is $1/(2n_pf_s)$, where f_s is the frequency of the source. Then, the on-time of the switches is calculated in each period. The converter current command is expressed from the vector diagram in Fig. 3 by

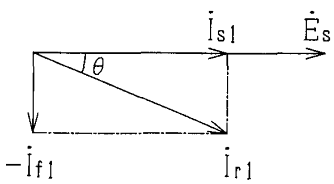

Fig. 3 Current vector

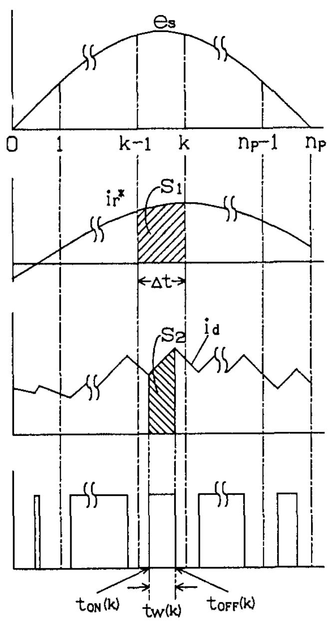

Fig. 4 Decision of on-time of switch

$$i_r^*(t) = \sqrt{2}\, I_r^* \sin(\omega_s t-\theta) \tag{2}$$

where

I_r^* an r.m.s. value of converter current command

Therefore, the area S_1 in Fig. 4 is obtained by

$$S_1 = \int_{(k-1)\Delta t}^{k\Delta t} i_r^*(t)dt = \pm\overline{i_r^*}(k)\,\Delta t \tag{3}$$

where

$\overline{i_r^*}(k)$ an average value of converter current command in the k-th period

S_1 is positive and the switches S_{w2} and S_{w3} act in the case of the plus sign in this equation. On the other hand, S_1 is negative and the switches S_{w1} and S_{w4} act in the case of the minus sign. Neglecting the resistance of the DC reactor because it has a high quality factor and assuming that the input terminal voltage of the converter is the source voltage, the increase of the current i_d during the switches conducting in the k-th period is expressed by

$$\Delta i_d^+(k) = \frac{\pm 1}{L}\overline{e_s}(k)t_w(k) \tag{4}$$

where

L an inductance of the reactor

$\overline{e_s}(k)$ an average value of the source voltage in the k-th period

$t_w(k)$ an on-time of the switches

The decrease of the current i_d during the switches non-conducting in the same period is expressed by

$$\Delta i_d^-(k) = -\frac{1}{L}\overline{v_c}(k)\{\Delta t-t_w(k)\} \tag{5}$$

where

$\overline{v_c}(k)$ an average value of the capacitor voltage in the k-th period

Therefore, the value of the current $i_d(k)$ is obtained from eqs.(4) and (5) at the (k-1) point as follows;

$$i_d(k) = i_d(k-1) + \frac{1}{L}[\pm\overline{e_s}(k)t_w(k) - \overline{v_c}(k)\{\Delta t-t_w(k)\}] \tag{6}$$

where

$i_d(k-1)$ a detected value of the reactor current

Then, the area S_2 shown in Fig. 4 is obtained by

$$S_2 = \frac{i_d(k-1) + i_d(k)}{2}\, t_w(k) \tag{7}$$

Thus, the on-time of the switches in the k-th period is decided by equaling the area S_1 and S_2.

$$S_1 = S_2 \tag{8}$$

Substituting eqs.(3), (6) and (7) into eq.(8), we obtain the next equation.

$$\frac{1}{2L}\{\pm\overline{e_s}(k) + \overline{v_c}(k)\}t_w(k)^2 + \{i_d(k-1) - \frac{\overline{v_c}(k)\Delta t}{2L}\}t_w(k) \mp \overline{i_r^*}(k)\Delta t = 0 \tag{9}$$

This is a quadratic equation with a variable of $t_w(k)$. Therefore, there are two solutions in eq.(9). However, $t_w(k)$ must satisfy the next expression.

$$0 \leq t_w(k) \leq \Delta t \tag{10}$$

Then, the only one solution is available.

$$t_w(k) = \frac{-b + \sqrt{b^2+4ac}}{2a} \tag{11}$$

where

$$a = \frac{1}{2L}\{\pm\overline{e_s}(k) + \overline{v_c}(k)\}$$

$$b = i_d(k-1) - \frac{\overline{v_c}(k)\Delta t}{2L}$$

$$c = \pm\overline{i_r^*}(k)\Delta t$$

Therefore, the switch-on and -off time of the switches are expressed by

$$t_{on}(k) = (k-0.5)\Delta t - t_w(k)/2 \tag{12}$$

$$t_{off}(k) = (k-0.5)\Delta t + t_w(k)/2 \tag{13}$$

In the proposed method, $\overline{e_s}(k)$ and $\overline{i_r^*}(k)$ is assumed by

$$\overline{e_s}(k) = \sqrt{2}\, E_s \sin\{\omega_s(k-0.5)\Delta t\} \tag{14}$$

$$\overline{i_r^*}(k) = \sqrt{2}\, I_r^* \sin\{\omega_s(k-0.5)\Delta t-\theta\} \tag{15}$$

where
E_s an r.m.s. value of the source voltage
Further, $\overline{v_c}(k)$ is approximated to be a value of the capacitor voltage at the k-th point, $v_c(k)$.

ANALYSIS OF CONVERTER PERFORMANCE

Waveforms

Fig. 5 shows the voltage and current waveforms. The circuit constants and the condition are listed in Table 1. The current command I_s^* is 2.0 Amp.

The waveform of the source current agrees well with the current command waveform although it has the ripples due to the PWM performance. The waveforms of the reactor current is a DC one with a small ripple due to the PWM performance and a large ripple synchronized with the source voltage. The waveform of the filter capacitor voltage is similar to the source voltage although it has a ripple due to the PWM performance.

Fig. 6 shows the source current waveform for the same condition in Literature [6]. The source current is a quasi-sinusoidal waveform with a ripple due to the PWM performance. However, it is leading to the source voltage because of the leading filter current. Therefore, the proposed strategy is proved effective for the improvement of the displacement power factor and the input power factor.

The Fourier series of the current is expressed by

$$i_s(t) = \sum_{n=1}^{\infty} \sqrt{2}\, I_n \sin(n\omega_s t-\phi_k) \tag{16}$$

where
I_n an r.m.s. value of the n-th harmonic
ϕ_n a phase of the n-th harmonic
Fig. 7 shows the harmonics of the source current i_s and the converter current i_r in Fig. 5. The fundamental component of the source current is 2.0 Amp. in accordance with the current command. The converter current has the harmonics around the integral multiple of the modulation frequency. As the high-order harmonics can be attenuated by the filter, only the 39th and the 41th harmonics remain a little in the source current. The harmonics due to the resonant frequency of the input filter generate in the source current, that is the 9th and the 11th harmonics. However, their amplitudes are very small compared with the fundamental component.

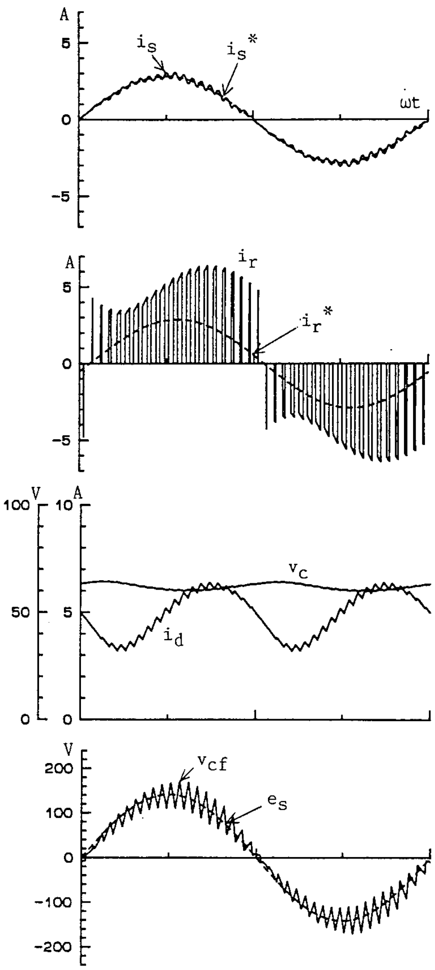

Fig. 5 Voltage and current waveforms

Table 1 Circuit constants

AC source	E_s	100.0 V
	f_s	60.0 Hz
Input filter	ω_0	$9.5\omega_s$
	L_f	7.8 mH
	R_f	0.29 Ω
	C_f	10.0 μF
DC reactor	L	50.0 mH
	Q_L	100.0
Capacitor	C	1000.0 μF
Load	R_L	20.0 Ω
	L_L	10.0 mH
Division of half cycle	n_p	20

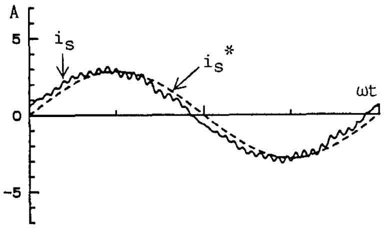

Fig. 6 Source current waveform in Literature [6]

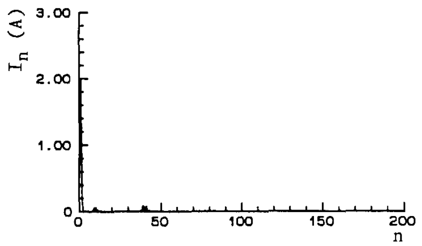

(a) source current

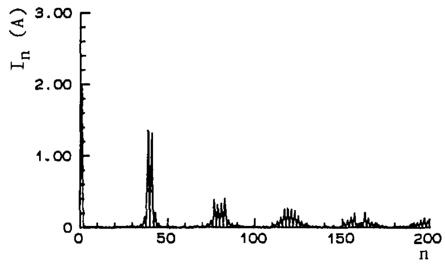

(b) converter current

Fig. 7 Harmonics of current

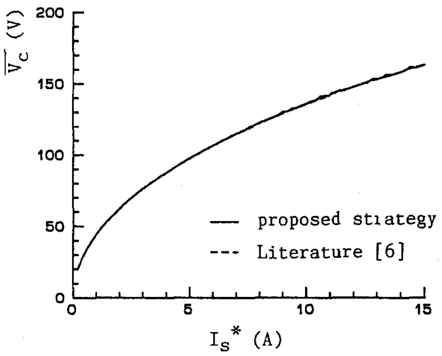

Fig. 8 Control characteristics of DC voltage

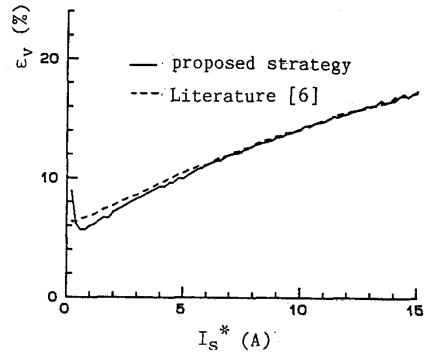

Fig. 9 Ripple factor characteristics

Control Characteristics of DC Voltage

Fig. 8 shows the control characteristics of DC voltage (the average value of DC voltage $\overline{V_c}$) with the circuit constants listed in Table 1. The DC voltage is regulated from zero to more than the maximum value of the source voltage by changing the current command. The control characteristics of DC voltage obtained in this paper is the same as those in Literature [6].

Fig. 9 shows the ripple factor characteristics with the circuit constants in Table 1. The ripple factor is expressed by the next equation.

$$\varepsilon_v = \frac{V_{cmax} - V_{cmin}}{\overline{V_c}} \times 100 \tag{17}$$

where

V_{cmax} the maximum value of DC voltage

V_{cmin} the minimum value of DC voltage

The ripple factor is almost the same as that in Literature [6]. It is less than about 18 %.

Input Characteristics

The displacement power factor, the distortion factor and the input power factor are discussed as the input characteristics. The Fourier analysis of the source current is expressed as eq.(16). Therefore, the displacement power factor (DPF), the distortion factor (DF) and the input power factor (PF) are expressed by

$$DPF = \cos(\phi_1) \tag{18}$$

$$DF = \frac{\sqrt{\sum_{n=2}^{\infty} I_n^2}}{I_1} \tag{19}$$

$$PF = \frac{1}{\sqrt{1 + DF^2}} \cos(\phi_1) \tag{20}$$

where

ϕ_1 a phase angle between the source voltage and the fundamental component of the source current

Fig. 10 shows the input characteristics with the circuit constants in Table 1. DPF is always an unity for all the current command as expected. On the other hand, DPF in Literature [6] is less than 1.0 in the small current command. The improvement of DPF can be achieved by the control method proposed in this paper.

DF is almost the same in the region of the current command above 1.0 Amp. However, DF for the proposed strategy is larger than that in Literature [6] in the small current command under 1.0 Amp. Consequently, PF for the proposed strategy is improved compared with that in Literature [6] and it is an unity in the almost region of current command.

CONCLUSIONS

The modified PWM control strategy in the single-

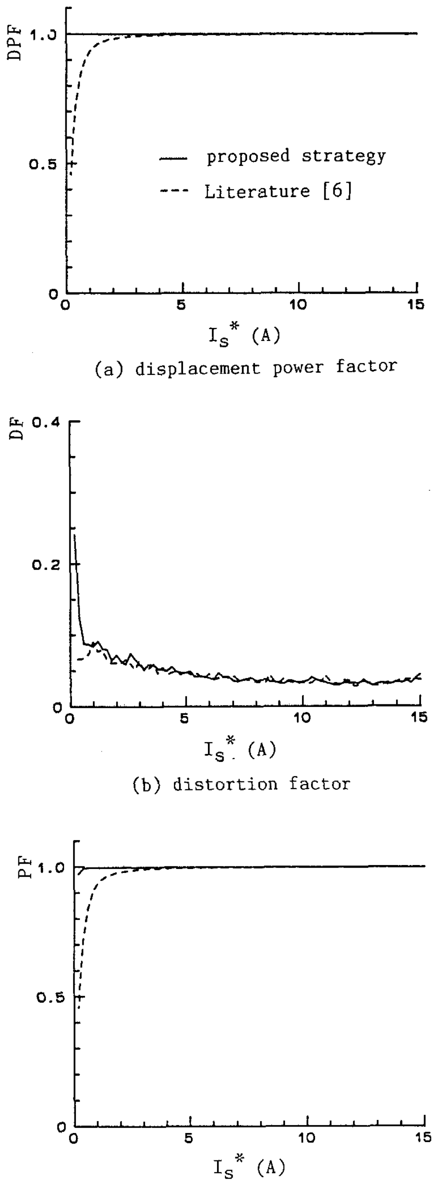

(a) displacement power factor

(b) distortion factor

(c) input power factor

Fig. 10 Input characteristics

phase AC to DC converter is proposed for the improvement of the displacement power factor and the input power factor. The validity of the proposed control strategy is clarified comparing with the characteristics in Literature [6] by simulation. It is found that the displacement power factor is an unity in the whole range of current command and the distortion factor is almost the same. Therefore, the input power factor is improved especially in the small range of current command and an unity in the wide range of current command.

REFERENCES

(1) T. Nishimura, T. Inoue, M. Nakaoka & T. Maruhashi : " Evaluation of Low Noise in Three Phase Induction Motor by Employing 20 kHz Carrier Sinusoidal PWM Inverter ", Trans. of IEEJ, Vol.107-D, No.5, p.620 1987

(2) H. S. Patel & R. G. Hoft : " Generalized Techniques for Harmonic Elimination and Voltage Control in Thyristor Inverters ; Part I - Harmonic Elimination ", IEEE Trans. Ind. Applic., Vol.IA-9, No.5, p.666 1973

(3) T. Kato & K. Iwamoto : " Optimum Pulse Pattern of Sinusoidal PWM Inverter with Filtering Effect ", Trans. of IEEJ, Vol.103-B, No.4, p.235 1983

(4) I. Takahashi & H. Mochikawa : " Optimum PWM Waveforms of an Inverter for Decreasing Acoustic Noise of an Induction Motor ", IEEE Trans. Ind. Applic., Vol.IA-22, No.5, p.828 1986

(5) Yoon-Jong Lee, Ki-Young Suh & Dong-Wha Chung : " Optimal PAWM strategy for variable speed drive of three phase induction motor ", Trans. Korea Inst. Electr. Eng. (South Korea), Vol.36, No.9, p.616 1987

(6) S. Funabiki & S. Matsuo : " Analysis of a PWM Controlled AC to DC Converter with a Controllability of DC Voltage and a High Input Power Factor ", Proc. IPEC Tokyo'90, Vol.1, p.505

(7) S. Fukuda & N. Tanaka : " PWM Technique for Current Source Converter ", 1987 National Conversion Record, IEE of Japan, Industrial Application, p.361